

# Synthesis and Characterization of Nickel Doped Urea Thiourea Naphthylamine Single Crystal Developed by Slow Evaporation Method

B. SENTHILKUMARAN<sup>1</sup>, S. ARIVOLI<sup>2\*</sup> and G. THANAPATHY<sup>3</sup>

<sup>1</sup>Department of Physics, Dharmapuram Adhinam Arts College,  
Dharmapuram, Mayiladudurai, India

<sup>2</sup>Department of Chemistry, Thiru Vi Ka Government Arts College, Thiruvarur, India

<sup>3</sup>Department of Physics, Poompuhar College, Sirkali, India  
*arivu6363@gmail.com*

Received 3 January 2017 / Accepted 20 January 2017

---

**Abstract:** A single crystal of nickel doped urea thiourea naphthylamine has been grown successfully from its aqueous solution. The grown crystals have been subjected to X-ray diffraction studies to identify the morphology and structure. The TGA studies showed the thermal properties of the crystals. The functional group of the grown crystals was identified by UV-Visible double beam spectra, FT-IR analysis, NMR and XRD studies.

---

**Keywords:** Urea, Thiourea, Naphthylamine, Nickel Sulphate, Nickel Naphthylamine Thiourea Urea single Crystal, X-Ray diffraction

## Introduction

Crystals are the essential pillars of modern technology. Without crystals, there would be no electronic and photonic industry, fibre optical communications, which depend on crystals such as semiconductors, superconductors, polarizers, transducers, radiation detectors, ultrasonic amplifiers, ferrites, magnetic garnets, solid state lasers, non-linear optics, electro-optic, acousto-optic, photosensitive, refractory of different grades, crystalline films for microelectronics and computer industries. Crystal growth is an interdisciplinary subject covering physics, chemistry, material science, chemical engineering, metallurgy, crystallography, mineralogy, *etc.* In the past few decades, there has been a growing interest on crystal growth processes, particularly in view of the increasing demand of materials for technological applications<sup>1-10</sup>. Atomic arrays that are periodic in three dimensions, with repeated distances are called single crystals. It is clearly more difficult to prepare single crystal than poly-crystalline material and extra effort is justified because of the outstanding

advantages of single crystals<sup>2</sup>. The reason for growing single crystals is, many physical properties of solids are obscured or complicated by the effect of grain boundaries. The chief advantages are the anisotropy, uniformity of composition and the absence of boundaries between individual grains, which are inevitably present in polycrystalline materials. The strong influence of single crystals in the present day technology is evident from the recent advancements in the above mentioned fields. Hence, in order to achieve high performance from the device, good quality single crystals are needed. Growth of single crystals and their characterization towards device fabrication have assumed great impetus due to their importance for both academic as well as applied research. To enable a material to be potentially useful for NLO applications, the material should be available in bulk single crystal form<sup>9</sup>. So, crystal growth of new nonlinear optical materials and investigation into their properties has become most indispensable and efficacious disciplines in the field of materials science and engineering. The rapid development of optical communication system has led to a demand for Nonlinear Optical (NLO) materials of high performance for use as components in optical devices. NLO materials are used in frequency conversion, which is a popular technique for extending the useful wavelength range of lasers. The search for new materials has identified novel semi organic systems of considerable potential and high performance<sup>10-21</sup>. There are three major stages involved in this research. The first is the production of pure materials and improved equipment associated with the preparation of these materials. The second is the production of single crystals first in the laboratory and then extending it to commercial production. The third is the characterization and utilization of these crystals in devices. In this paper, the method of crystal growth with emphasis on low temperature solution growth technique was described.

## Experimental

An essential prerequisite for success in crystal growth is the availability of material of the highest purity. Solute and solvents of high purity are required, since impurity may be incorporated into the crystal lattice resulting in the formation of flaws and defects. Sometimes impurities may slow down the crystallization process by being adsorbed on the growing face of the crystal, which changes the crystal habit. A careful repetitive use of standard purification methods of recrystallization followed by filtration of the solution would increase the level of purity.

### *Seed preparation*

0.80 g of urea, 1.15 g of naphthylamine, 0.9 g of thiourea and 1.08 g of nickel sulphate were dissolved in 30 mL of double distilled water. The solution was thoroughly mixed using a magnetic stirrer. A crystalline substance was formed. The urea, thiourea, naphthylamine, nickel sulphate solution were prepared in water and maintained at 30 °C with continuous stirring to ensure homogeneous temperature and concentration. The solution was kept at 30 °C for ten days in order to get the nickel doped naphthylamine thiourea and urea doped single crystal.

Crystal growth of large single crystals can be grown from slow evaporation solution growth. Single crystals of nickel doped naphthylamine thiourea and urea are grown by slow evaporation of the saturated aqueous solution at room temperature. Good quality single crystals were grown within ten days (Figure 1).





**Figure 1.** Photograph of NiNTU

## Results and Discussion

### *X-Ray diffraction analysis*

Single crystal X-ray diffraction study was performed for the grown NiNTU crystal. It was found that NiNTU crystal belongs to orthorhombic system ( $\alpha = \beta = \gamma = 90^\circ$ ). Lattice parameter values of NiNTU are compared with reported NTU in Table 1. In the case of doped sample, a slight variation in the cell parameters is observed, which may be due to the incorporation of urea and thiourea ligands. This analysis reveals that the induction of urea and thiourea ligand in the NiNTU crystal does not change the crystal system though there is a small change in the lattice parameters. The powder sample of NiNTU was scanned over the range  $10\text{--}80^\circ$  at a rate of  $1^\circ$  per minute and the powder X-ray diffraction patterns were indexed using Check cell software (Figure 2). The lattice parameter ( $a$ ) was calculated by selecting the (102) plane using the formula<sup>2</sup>:

$$\sin^2\theta = \frac{\lambda^2}{4a^2} (h^2 + k^2 + l^2)$$

**Table 1.** Lattice parameter values of NiNTU and reported NTU crystals

Sample	System	2 $\theta$ (degree)	FWHM	hkl	Lattice parameter (Å)	
					Calculated	Reference[2]
NTU	Orthorhombic	23.25	0.16	200	7.644	7.644
		20.81	0.16	020	8.527	8.559
		32.57	0.24	002	5.493	5.492
NiNTU	Orthorhombic	28.6258	0.4040	200	3.1158	3.2041
		20.6166	0.4326	020	4.3046	4.3028
		22.9938	0.4553	002	3.8647	3.9865

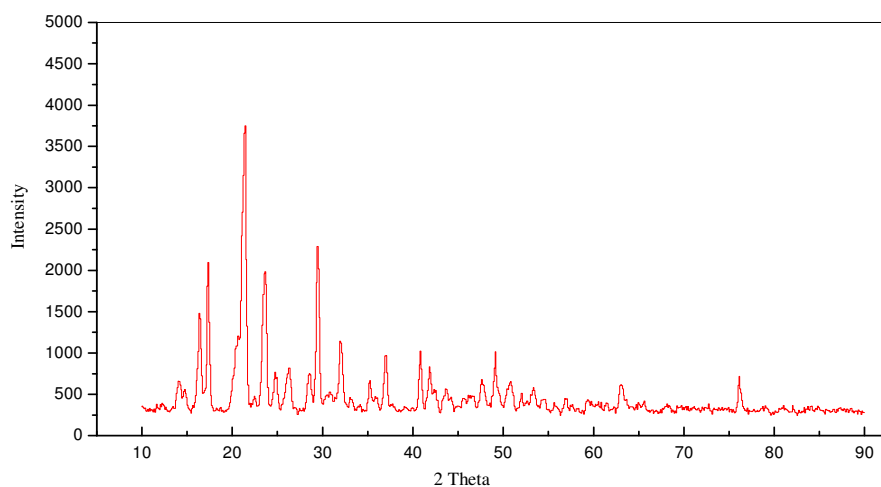


**Figure 2.** XRD pattern of NiNTU

### Fourier transforms infrared spectroscopy

The FT-IR spectra of nickel urea thiourea naphthylamine grown crystals are shown in Figure 3. In the higher wavelength region, the peak at 3500 is assigned to hydrogen bonding, the peak at 3480  $\text{cm}^{-1}$  is assigned to C-H, N-H stretching vibration. The region 3430  $\text{cm}^{-1}$  and 3120  $\text{cm}^{-1}$  with strong intensity represents N-H stretching mode. The broad envelope positioned in between 3420  $\text{cm}^{-1}$  and 2740  $\text{cm}^{-1}$  corresponds to the symmetric and asymmetric stretching modes of  $\text{NH}_2$  group. The peak at 2920-2880  $\text{cm}^{-1}$  with medium intensity refers C-H asymmetric stretching. Combinational overtones extend to the bands from 2420-2300  $\text{cm}^{-1}$ . The peak at 1750  $\text{cm}^{-1}$  indicating the C=O stretching mode of vibration. The  $\text{NH}_2$  bending vibrations occur at 1630, 1622 and 785  $\text{cm}^{-1}$ . The peak at 1540  $\text{cm}^{-1}$  is due to  $\text{NH}_2$  bending vibration. The peaks at 1490-1440  $\text{cm}^{-1}$  corresponds to the C=S stretching. The C-C stretching mode of vibration occurs in 1328  $\text{cm}^{-1}$  peak. The peak at 1225  $\text{cm}^{-1}$  gives rise to C-N stretching mode of vibration. The spectra show absorption bands in the region of 1145  $\text{cm}^{-1}$  and 1030  $\text{cm}^{-1}$  which are due to in-plane C-H bending vibration. The band 1115  $\text{cm}^{-1}$  signifies the N-H symmetric bending. The bands at 857  $\text{cm}^{-1}$  and 808  $\text{cm}^{-1}$  revealed that C-N deformation mode. The ring deformation occurs at 828  $\text{cm}^{-1}$ . C=O deformation is identified by the band at 675  $\text{cm}^{-1}$ . C-H out-of plane bending peaks obtained at 660  $\text{cm}^{-1}$  and 648  $\text{cm}^{-1}$ . The bands 645-638  $\text{cm}^{-1}$  represents C-C deformation. The absorption bands in the region of 486-471  $\text{cm}^{-1}$  are due to N-C stretching vibration. The assignments confirm the presence of various functional groups present in the material. The absorption around 1600  $\text{cm}^{-1}$  is  $\text{NH}_2$  bending and this band would be shifted into lower wavelength region 1638  $\text{cm}^{-1}$ . The absorption bands in the region of 920-810  $\text{cm}^{-1}$  are due to the presence of aromatic ring. Our investigations were well compared with earlier reports<sup>10-19</sup>.

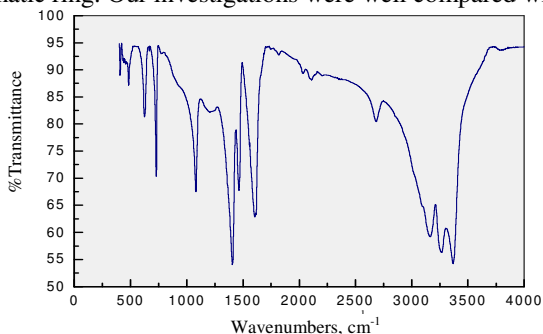


**Figure 3.** FT-IR spectrum of NiNTU

### UV- Visible studies

The UV-Visible spectrum of the single crystal NiNTU indicates low and high absorption in the entire visible and near infrared region of the crystals. This is a desirable property for NLO applications since a wider optical transparency in these regions enhances the frequency conversion efficiency in the corresponding wavelengths (Table 2).

The cut off wavelengths of NiNTU single crystal were found to be 480 nm, 866 nm, 920 nm, 974 nm and 1017 nm respectively. The presence of amino, imino, keto and thio carbonyl groups are confirmed by the peaks around 416, 480, 574 and 866 nm values. The presence of aromatic ring is confirmed by the cut of wavelength around 920, 975, 1017 nm. The good optical transmittance in the entire visible region and the cut off wavelength ( $\lambda_{\text{cut}}$ ) was observed as this is due to  $\pi$ - $\pi^*$  transition in the compounds. The band gap energy ( $E_g = hc/\lambda$ ) was found to be 10.46 eV for pure and NiNTU crystals. The large transmission in the entire visible region and short cut off wavelength enables it to be a potential material for second and third harmonic generation<sup>20-27</sup>.

**Table 2.** Cuts off wavelengths of NiNTU single crystal

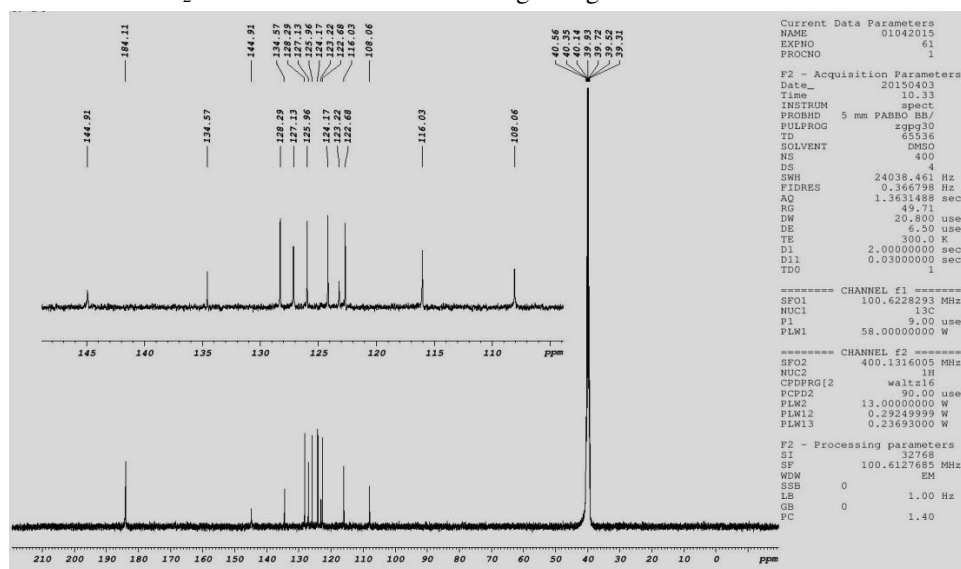
Crystal	Wavelength, nm	% Transmittance
NiNTU	416	57.0
	480	57.1
	574	59.2
	866	92.9
	920	91.9
	974	136.1
	1017	102.9

### Nuclear magnetic resonance spectroscopy

NMR spectrum of NiNTU was recorded using FT-NMR spectrometer. NiNTU crystal was powdered and dissolved in deuterated dimethyl sulfoxide (DMSO). FT-NMR spectrum recorded for NiNTU is shown in Figure 4. A chemical shifts at 8.230, 8.024, 7.698 and 7.067 ppm are due to Ar-H in the form of bicyclic ring proton. The chemical shift at 7.047 – 7.716 ppm is assigned to =C-NH-C= proton. Chemical shift at 6.647 – 6.665 ppm is due to H-N-C=O. A chemical shift at 5.522 – 5.626 ppm is due to naphthylamine proton<sup>12</sup>. The chemical shift at 7.323-7.7.406 is due to H-N-C=O. A chemical shift at 3.460 is due to -C=S. The above values confirm the structure of NiNTU.

### Thermal analysis

TGA analysis of the NiNTU crystal was carried out in the temperature range 10- 900 °C. The recorded thermogram is shown in Figure 5. From TGA curve it is observed that the weight loss start from 220°C. There is 35.5 % weight loss is due to the liberation of naphthylamine molecule at 240°C. There is 6.56 % weight loss between 330 °C to 390 °C. This weight loss is due to the liberation of NH<sub>3</sub>. There is 11.5 % weight loss between 590°C to 670°C. This weight loss is due to the liberation of CO. There is 13.4 % weight at 830°C. This weight loss is due to the liberation of H<sub>2</sub>S. This endothermic event is in good agreement with the TGA trace<sup>21</sup>.

**Figure 4.** NMR spectrum of NiNTU

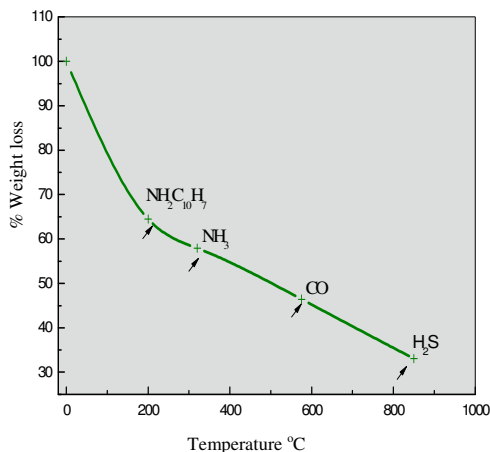


**Figure 5.** Thermogravimetric analysis for the determining the weight loss

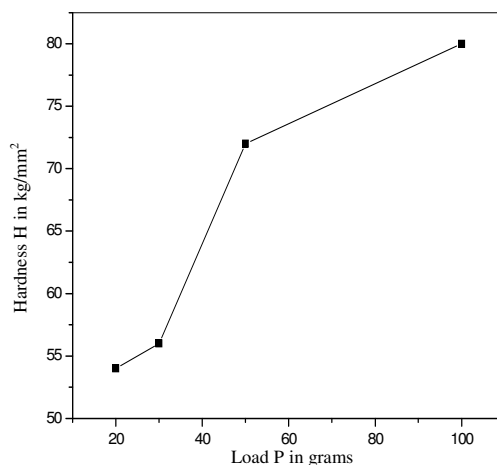


**Figure 6.** Variation hardness number with load

### Micro hardness studies

Hardness of the material is a measure of resistance that offers to deformation. The transparent polished crystal free from cracks was selected for hardness measurements. The indentations were made on the flat surface with the load ranging from 10 to 100 g using Shimadzu make-model-HMV-2 fitted with Vicker's pyramidal indenter and attached to an incident light microscope. The indentation time was kept as 5s for all the loads. The Vicker's hardness (Hv) was calculated from the relation<sup>21</sup>

$$Hv = \frac{1.8544P}{d^2} P / d^2 \text{ kg / mm}^2$$

Where, P is the applied load and d the average length of the diagonal of the indentation mark. With P in g and d in  $\mu\text{m}$ , the units of Hv turned out to be  $\text{kg/mm}^2$ . The variation of micro hardness with applied load for the prominent (102) plane of the NiNTU crystal is shown in Figure 6. It is found that the hardness values increases with the increase of the applied load. This behaviour of increasing micro hardness with the load known as reverse indentation size effect (RISE)<sup>21</sup>, which is also attributed due to existence of distorted zone near crystal medium interface, effect of vibrations, specimen chipping *etc.*, and the plastic deformation is dominant. At low loads or strains, plastic deformation of crystals mainly involves the nucleation of dislocations along a particular slip system. The RISE effect can be qualitatively explained on the basis of the depth of penetration of the indenter<sup>21</sup>. At small loads, the indenter penetrates only the surface layers and therefore, the effect is shown sharply at the early stages. When the applied load increases, the penetration depth also increases and the overall effect must be due to the surface and inner layers. When only one slip system is active during plastic deformation at low loads, the number of active parallel glide planes during indentation is low. Therefore the nucleating dislocations rapidly propagate into the material without experiencing substantial mutual interaction stress between them. Consequently in this stage, indentation depth increases proportionally with applied pressure.

### NLO studies

The second harmonic signal, generated in the crystals was confirmed from the emission of orange radiation by the crystals. The NLO SHG values of the NiNTU single crystals were determined and compared to the reported SHG value of pure KDP<sup>21</sup> is shown in Table 3.

**Table 3.** The NLO SHG value of pure KDP

Crystal	Second harmonic signal output (mJ)	SHG efficiency (compared to SHG efficiency of pure KDP)
NiNTU	10.5	4.2

### Conclusion

The good quality single crystals of Nickel Naphthylamine Thiourea Urea single Crystal are successfully grown by slow evaporation method at room temperature. The UV-Visible spectra showed that the crystals had a wide optical window, no absorbance and good optical transmittance in the entire visible region. FT-IR analysis confirmed the presence of functional groups in the grown crystals. TGA thermogram revealed the thermal stability of the materials. The powder X-Ray diffraction study confirms the lattice parameter values. The good optical quality and their suitability for NLO applications. Kurtz-Perry powder SHG test was employed to determine the SHG efficiency of the samples and the values were compared to the reported SHG efficiency of pure KDP.

### References

1. Saha J K and Podder J, *J Bangladesh Academy of Sciences*, 2011, **35(2)**, 203-210; DOI:10.3329/jbas.v35i2.9426
2. Viruthagiri G, Praveen P, Mugundan S and Anbuvaran M, *Indian J Adv Chem Sci.*, 2013, **1(4)**, 193-200.
3. Sundararajan R S, Senthilkumar M and Ramachandraraja C, *J Crystallization Process Technology*, 2013, **3**, 56-59; DOI:10.4236/jcpt.2013.32008
4. Gunasekaran S, Anand G, Arun Balaji R, Dhanalakshmi J and Kumaresan S, *J Phys.*, 2010, **75(4)**, 683-690; DOI:10.1007/s12043-010-0148-y
5. Thomas Joseph Prakash J and Ruby Nirmala L, *Inter J Compr Appl.*, 2011, **6**, 0975-8887.
6. Duan X E, Wei X H, Tong H B, Bai S D, Yong B Z and Dian S L, *J Mole Struct.*, 2011, **1005(1-3)**, 91-99; DOI:10.1016/j.molstruc.2011.08.030
7. KrishnaMoha M N, Jagannathan K, Ponnusamy S and Muthamizhchelvan C, *J Phys Chem Solids*, 2011, **72(11)**, 1273-1278; DOI:10.1016/j.jpics.2011.07.020
8. Muthu K and Meenakashisundaram S P, *J Crystal Growth*, 2012, **352(1)**, 158-162; DOI:10.1016/j.jcrysgro.2012.01.024
9. Chandrasekaran J, Ilayabarathi P, Maadeswaran P, Mohamed Kutty P and Pari S, *Optics Commun.*, 2012, **285(8)**, 2096-2100; DOI:10.1016/j.optcom.2011.12.063
10. Chandrasekaran J, Ilayabarathi P and Maadeswaran P, *Rasayan J Chem.*, 2011, **4(2)**, 320-326.
11. Krishnakumar V and Nagalakshmi R, *Spectrochimica Acta Part A: Molecular Biomolecular Spectroscopy*, 2007, **68(3)**, 443-453; DOI:10.1016/j.saa.2006.11.049
12. Vijayan N and Ramesh Babu R, *J Crystal Growth*, 2004, **267(3-4)**, 646-653; DOI:10.1016/j.jcrysgro.2004.04.008
13. Mohankumar R and Rajanbabu D, Jayaramanc D, Jayavel R and Kitamura K, *J Crystal Growth*, 2005, **275(1-2)**, 1935-1939; DOI:10.1016/j.jcrysgro.2004.11.260

14. Merry H O, Warren L F, *Applied Optics*, 1992, **31(24)**, 5051-5060; DOI:10.1364/AO.31.005051
15. Venkataraman V, Dhavaraj G and Bhat H L, *J Crtyz Growth*, 1995, **154(1-2)**, 92-97; DOI:10.1016/0022-0248(95)00212-X
16. Hanna M C, Lu Z H, Cahill A F, Heben M J and Nozik A J, *J Crystal growth*, 1997, **174(3-4)**, 605-610; DOI:10.1016/S0022-0248(97)00029-8
17. Cu D, Jiaog M and Taus Z, *Acta Chimica Sinica*, 1983, **41(6)**, 570-573.
18. Ramachandraraja C and Sundararajan R S, *SpectrochimicaActa Part A: Molecular Biomolecular Spectroscopy*, 2008, **71(4)**, 2008, 1286-1289; DOI:10.1016/j.saa.2008.03.028
19. Kurtz S K and Perry T T, *J Appl Phys.*, 1968, **39(8)**, 3798-3814; DOI:10.1063/1.1656857
20. Martin Britto Dhas S A, Suresh J, Bhagavannarayana G and Natarajan S, *Open Crystallography J*, 2008, **1**, 46-50; DOI:10.2174/1874846500801010046
21. Ruby A and Alfred Cecil Raj S, *International J Scientific Res Publications*, 2013, **3(3)**, 1-5.
22. Lawrence G M and Thomas Joseph Prakash J, *Spectrochimica Acta Part A*, 2012, **91**, 30-34; DOI:10.1016/j.saa.2012.01.055
23. Patel J D, Mighri F and Ajji A, *Materials Letters*, 2012, **74**, 183-186; DOI:10.1016/j.matlet.2012.01.089
24. Patel J D, Mighri F, Ajji A and Chaudhurid T K, *Mater Chem Phys.*, 2012, **132(2-3)**, 747-755; DOI:10.1016/j.matchemphys.2011.12.006
25. Anandan P, Jayavel R, Saravanan T, Parthipan G, Vedhi C and Mohan Kumar R, *Optical Materials*, 2012, **34(7)**, 1225-1230; DOI:10.1016/j.optmat.2012.01.042
26. Joema S E, Perumal S and Ramalingam S, *Recent Res Technol.*, 2011, **3**, 2076-5061.
27. Ramajothi J, Dhanuskodi S and Akkurt M, *Spectrochimica Acta Part A*, 2008, **69(4)**, 1271-1276; DOI:10.1016/j.saa.2007.07.019